

Mechanical behaviour and morphology of tactic poly(vinyl methyl ether)/polystyrene blends*

G. Beaucage† and R. S. Stein

Department of Polymer Science and Engineering, University of Massachusetts, Amherst, MA 01003, USA

(Received 11 February 1993; revised 18 October 1993)

The mechanical properties of tactic poly(vinyl methyl ether)/polystyrene (PVME/PS) blends are investigated as a route to toughened polymers by using the lower critical solution temperature (*LCST*) behaviour as a mechanism for the production of rubbery domains. Crystallites in the tactic PVME-rich phase act as physical crosslinks. Shear bands as well as crazes are observed in these *in situ* composites due to interaction between a PS matrix plasticized with PVME and the PVME-rich rubbery domains.

(Keywords: blends; polystyrene; poly(vinyl methyl ether))

INTRODUCTION

The production of an impact resistant glassy polymer through the addition of an elastomer has been approached via a myriad of techniques. Bucknall¹ has extensively discussed the details of this technology. The most direct approach to the production of a high-impact material would seem to be the bulk mixing of rubbery and glassy polymers. In general, this results in a composite material with drastically reduced modulus, strength and impact properties. The rubber particles in such a bulk mixture separate easily from the glassy matrix, producing voids which lead to failure at low stresses. Thus, one is incipiently faced with the problem of interfacial adhesion and miscibility between the elastomer and glass. For styrenic polymer mixtures²⁻¹³ this is commercially circumvented through the chemical grafting of the glassy component to the rubbery component of an immiscible mixture. High-impact polystyrene (HIPS), for example, is produced industrially from a solution of butadiene rubber in styrene monomer. Polymerization of styrene results in phase separation of the two immiscible polymers. When the volume percentage of the polystyrene exceeds that of the polybutadiene, phase inversion occurs, wherein the matrix phase shifts from polybutadiene to polystyrene. The rubbery domains consist of roughly spherical particles with diameters greater than 2 μm . A distribution of rubber particle sizes is observed. Vigorous mixing of the ternary mixture during phase inversion results in polystyrene inclusions in the rubbery domains. This serves to further improve the impact properties by increasing the volume of the suspended rubbery domains,

the surfaces of which act to initiate and/or terminate stress relieving crazes.

Crazes are the predominant mechanism of stress abatement in HIPS. Elastic deformation of the rubber may also be a factor. In other toughened styrenic mixtures, such as PS/poly(phenylene oxide) and PS block copolymers with butadiene, shear bands may occur, together with crazes. Generally it is observed that the presence of shear bands tends to inhibit the formation and growth of crazes¹. Shear bands appear to be a more important mechanism of stress relief in systems where the matrix component is less brittle, such as toughened poly(vinyl chloride) (PVC) and polycarbonate.

In the manufacture of toughened PVC¹⁴⁻¹⁹ a rubber with a solubility parameter close to that of PVC, such as nitrile rubber i.e. poly(butadiene-*co*-acrylonitrile), is melt blended with PVC. The rubber is partially compatible with PVC and a fine dispersion of the rubber results. The rubbery dispersion has good interfacial properties. Similarly, toughened polypropylene^{20,21} can be made by the direct melt blending of polypropylene with ethylene propylene diene rubber.

Another approach to reinforcement in styrenics involves the use of block copolymers^{5,22,23} such as poly(styrene-*b*-butadiene) (SBR), resulting in intimately bound rubbery domains. Durst *et al.*²⁴ report that a maximum in impact strength occurs in these systems when the fraction of butadiene in the block copolymers approaches 50 wt%.

In the present study, a rubber modified glassy polymer is produced through the phase separation of a miscible rubbery/glassy blend at elevated temperatures, followed by quenching of the glassy phase below the glass transition temperature (T_g)²⁵. Under ideal thermal cycling conditions, rubber particles of optimal size, intimately interfaced with the glassy matrix, are produced. The domain size and composition of the rubbery and glassy phases are under experimental control.

* Supported in part by a grant from Polysar Incorporated, now a division of NOVA Corporation

† To whom correspondence should be addressed. Present address: Group 1815, Sandia National Laboratory, Albuquerque, NM 87185, USA

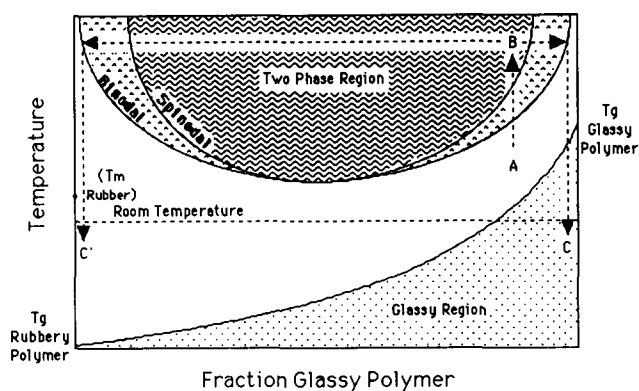


Figure 1 Ideal phase diagram for the production of a rubber toughened glassy polymer through controlled phase separation

In order to manipulate the morphology of a simple binary polymer blend we require a phase diagram of the type shown in *Figure 1*. For such an ideal system, the phase-separated morphology can be controlled, and to some extent predicted, by the careful manipulation of processing conditions. Following the dashed line shown in *Figure 1*, the temperature of the blend is raised above the glass transition temperature of both components and is processed as a miscible melt (A). After the first phase of processing is complete, the blend can be thermally cycled above the binodal (and optionally above the spinodal temperature (B)) in order to effect a partial degree of phase separation for toughening. Rapid quenching of a stoichiometrically optimal blend results in a glassy matrix (C) with an intimately interfaced, rubbery suspension (C'). The extent of interaction at the interface is controlled through the manipulation of the residence time above the binodal and/or spinodal temperatures. In more complicated phase diagrams other morphological characteristics of the material, such as the crystallinity of the glassy and rubbery components, can also be thermally controlled. The mechanical properties of blends, phase separated in the binodal, may differ from those separated in the spinodal, due to differences in morphology. However, the border between the spinodal and the binodal regions, defined by the Flory-Huggins theory, is not well defined in practice.

The production of a rubbery phase requires crosslinks. These can be produced by chemically crosslinking the rubbery phase after phase separation has occurred. Alternatively, physical crosslinks can be induced in the rubbery phase. A high-molecular-weight rubbery material, for example, exhibits entanglements which can act as physical crosslinks at the high strain rates which are present in localized fracture phenomenon. However, high molecular weights are known to dramatically shift the miscibility. Physical crosslinks can also be produced in chemically tailored block copolymers. However, the simple phase diagram of *Figure 1* becomes quite complex in this case.

In this study we use a limited degree of crystallinity in the rubbery phase to induce physical crosslinks. The melting point is denoted as T_m on the y -axis of *Figure 1*. 10% crystallinity will produce close to an optimal rubber. From previous studies²⁶⁻³⁰ it is known that large changes in tacticity which lead to crystallinity have relatively minor effects on the phase diagram. For monosubstituted

vinyl polymers a 10 to 20°C shift in the cloud point temperature is observed with tacticity changes²⁷.

The PS/PVME (polystyrene/poly(vinyl methyl ether)) system is used as a model system which produces the salient behaviour of *Figure 1*. This is chosen because its phase behaviour is well characterized and because polystyrene is commercially available as monodisperse or bulk polydisperse samples. The large index of refraction difference between the two polymers allows for optical determination of the phase diagram²⁶⁻²⁹. Furthermore, the availability of deuterated PS allows for more elaborate studies of the miscibility, involving neutron scattering³⁰ and reflection³¹. *i*PVME (isotactic PVME), which is not commercially available, shows a partial degree of crystallinity, usually close to 10% (as polymerized). The material forms imperfect crystallites which are detected by X-ray diffraction, differential scanning calorimetry (d.s.c.) and other techniques, such as measurement of the index of refraction²⁶. *i*PVME with about 10% crystallinity is a rubbery material with a T_g of approximately -30°C , making it less than optimal for a commercial rubber but sufficiently rubbery for the purposes of an academic study.

A preliminary study of miscibility in the *i*PVME/PS system was reported by Bank *et al.*³² involving the study of high-molecular-weight *i*PVME (650 kg mol^{-1}), which has a relatively low degree of isotacticity. These authors found that this material shows some unspecified degree of miscibility with polystyrene. Previous studies³³⁻³⁵ indicate that atactic PVME above 600 kg mol^{-1} , blended with PS in the 100 kg mol^{-1} range, is immiscible above the glass transition temperature of a 10 wt% PVME blend due to strong molecular-weight effects in this system. The blends produced by Bank and coworkers are probably in the immiscible region. Generally, the phase behaviour of the atactic system exhibits a lower critical solution temperature ($LCST$) similar to that in *Figure 1*. *i*PVME shows similar phase behaviour to atactic PVME with a somewhat reduced miscibility (see later). The miscibility limits for moderate-molecular-weight isotactic PVME/PS occur at convenient temperatures for study and are well within the temperature scheme specified in *Figure 1*.

In this study, a moderate-molecular-weight PVME (99 kg mol^{-1}) is used in order to widen the miscibility window. This polymer has a much higher degree of isotacticity (70% isotactic triads) than the material used by Bank *et al.* so that a higher density of physical crosslinks occurs, making the material more resilient. The atactic material is a viscous liquid. In contrast, the crystalline isotactic material is a rubber with thermally removable, physical crosslinks, specifically the *i*PVME crystallites. Above the crystalline melting point, isotactic and atactic PVME are optically and mechanically indistinguishable. These two tactic forms have identical glass transitions³⁶.

Solution-cast samples of *i*PVME/PS phase separate due to crystallization of the *i*PVME. A clearing point is observed as reported in ref. 28. The difference in mechanical properties between this crystallization-driven phase separation and thermally induced phase separation is discussed below. Generally, fractionation by molecular weight occurs in thermally induced phase separation, as discussed in ref. 29. Synthesis of *i*PVME was carried out by the present authors at Polysar Ltd's pilot plant in Sarnia, Ontario (now a division of Nova

Corporation), and on a laboratory scale at the University of Massachusetts²⁶⁻³⁰.

EXPERIMENTAL

Two types of mechanical test specimens are investigated. First, solution-cast rectangular films, ~ 0.05 – 0.1 mm thick, 0.5 cm wide and 6 cm in length, which are produced by solvent casting of 15 wt% PVME blends from toluene at room temperature on Teflon sheets. A total polymer content of 20 wt% is used. The films are allowed to air dry for at least three days, followed by drying in a vacuum oven at $\sim 35^\circ\text{C}$ for at least three weeks. After vacuum drying the samples are dried in the dark under ambient conditions for at least one further week. This procedure removes essentially all of the toluene from the blends. Gas chromatography fails to resolve any residual toluene in the cast samples. These solution-cast samples are reproducible. Furthermore, samples stored under ambient conditions in the dark for several months show no change in mechanical properties.

In these solution-cast samples, phase separation occurs due to crystallization of the iPVME from solution as the toluene evaporates. X-ray diffraction from these blends indicates the presence of a slight degree of crystallinity. Because of the low overall degree of crystallinity (i.e. 15% PVME $\times 10\%$ crystallinity = 1.5% total crystallinity in the blends), an absolute determination of the degree of crystallinity cannot be made. For similar blends having higher percentages of PVME we estimate approximately 10% crystallinity in the PVME phase from X-ray diffraction studies. An attempt was made to induce thermal phase separation after annealing away the phase separated structure in these blends. However, due to the thinness of the films, inhomogeneities result, which make mechanical testing of thermally treated films impossible.

Mechanical tests were performed on the as-cast films described above. PVME phase sizes of 1 – $25\ \mu\text{m}$ are observed in the solution crystallized blends by light scattering, optical microscopy and transmission electron microscopy (TEM).

The second type of mechanical test sample is a melt blended ASTM standard sample. These were produced after large quantities of iPVME were synthesized at Polysar Ltd's Sarnia, Ontario pilot plant (now a division of NOVA Corporation) by the authors. Melt blended materials were produced at Polysar's Leominster, MA facility, using a Brabender[®] mixer of 50 g capacity, in the miscible region ($\sim 120^\circ\text{C}$). These blends were ground and pressed under vacuum into dog-bone shaped tensile bars according to ASTM standards (ASTM standard D 638 Type V) at temperatures above the cloud point of the blend ($\sim 156^\circ\text{C}$). The melt blended 'dog-bones' are 0.24 cm thick and 0.32 cm wide at the centre, with a gauge length of 1.27 cm.

Different stress/strain conditions may exist in the two sample types. For example, in the limit of an extremely thin sample, plane stress conditions exist in a tensile experiment, since a very thin sheet of material can contract volumetrically. Under these conditions dilatational strain is minimized. Crazeing is a dilatational deformation, i.e. localized volumetric strains occur. A craze is a localized region of lower density. Shear banding, on the other hand, occurs in the absence of volumetric changes. Therefore, in very thin samples, one is more likely to observe shear banding, rather than crazeing. At

the opposite extreme, i.e. a very thick specimen, plane strain conditions exist at the centre of the specimen, causing large amounts of dilatational strain which favour crazeing. The samples discussed above lie between these two extremes.

RESULTS AND DISCUSSION

Solution-cast samples

Figure 2 shows four typical stress/strain plots for solution-cast PVME/PS blends, and also one of an identically produced HIPS sample for comparison. The curves are shifted along the strain axis in order to facilitate comparison. All of the tensile tests are performed under a constant strain rate of $10\ \text{mm min}^{-1}$. The stress values shown in Figure 2 are not comparable on an absolute scale with values obtained from ASTM standard samples since mechanical properties vary with sample dimensions and non-standard dimensions are used out of necessity. However, comparison of general features and comparison with similarly dimensioned samples is appropriate.

Figure 2a shows a typical tensile test for a pure polystyrene cast film of $120\ \text{kg mol}^{-1}$. Brittle failure occurs at about 1.6% strain. Figure 2b is a typical tensile test for a miscible blend of 15 wt% atactic, non-crystalline PVME of $99\ \text{kg mol}^{-1}$, blended with PS. This blend is a single phase. Brittle failure occurs after about 3% strain. The initial modulus, i.e. the initial slope of the stress/strain plot, is reduced for the atactic blend when compared with pure PS. Figure 2c is an isotactic PVME blend of the same composition which contains large crystalline domains of $\sim 25\ \mu\text{m}$ diameter. Brittle failure occurs after a small degree of strain. The initial modulus is not significantly different from that of PS, indicating that the matrix is predominantly PS, with most of the PVME presumably being tied up in crystalline domains. Figure 2d is a 15 wt% blend of isotactic PVME with PS having crystalline domains of ~ 1 – $5\ \mu\text{m}$. A significant increase in the strain at failure occurs in this material. A broad yield point is observed and failure is by a ductile mechanism. The initial modulus is reduced in this case when compared with Figures 2c and 2a, but is not as low as the non-crystalline, single-phase atactic blend of Figure

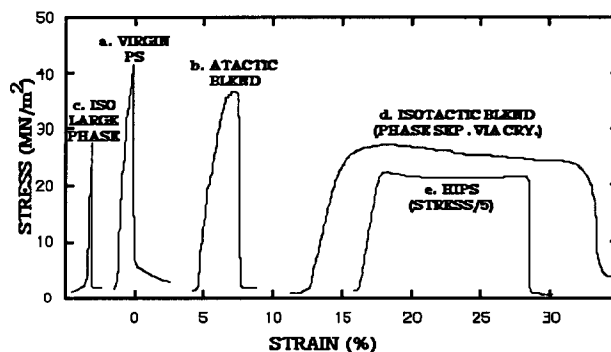


Figure 2 Typical stress/strain plots for solution-cast samples: (a) a typical tensile test for a pure polystyrene cast film; (b) a typical tensile test for a miscible blend of 15 wt% atactic PVME/PS; (c) an isotactic PVME blend of the same composition with large crystalline domains ($25\ \mu\text{m}$); (d) a 15 wt% blend of isotactic PVME with PS having crystalline domains of $\sim 5\ \mu\text{m}$ and; (e) a film sample of Polysar HIPS. All materials are prepared under the same conditions, and the curves are shifted along the strain axis in order to fit them all on to one plot. The stress scales are identical in all cases except for curve (e)

2b. The initial modulus indicates that the matrix phase in *Figure 2d* contains more PS than that in *Figure 2c*, but less than that of the atactic blend (*Figure 2b*).

Figure 2e shows similar stress/strain data for a cast film sample of Polysar HIPS. The behaviour of the sample of *Figure 2d* is similar to the behaviour of the HIPS sample. The yield stress for the HIPS film is close to 125 MN m^{-2} , while the isotactic PVME blend shows a lower yield stress of $\sim 35 \text{ MN m}^{-2}$. Due to the inherent variability in thickness, the small stresses measured and the inability to perform impact tests on the thin solution-cast films, it is impossible to obtain quantitative estimates of the energy absorbed, or the initial modulus of the solution-cast films, although the larger strain at failure of the isotactic PVME blend, i.e. $\sim 20\%$, in comparison with HIPS (12%), indicates a similar or larger total energy absorption.

Qualitatively, one may compare the tensile stress/strain curves of HIPS and *Figure 2d*. HIPS shows a very linear region at the onset of stress, with a modulus similar to that of pure PS. This indicates that the matrix phase is not significantly plasticized by the immiscible rubber inclusions. The linear elastic region is followed by a yield point. This is explained³⁷ as resulting from a minimum stress value for the initiation of crazing, as well as a minimum time period. Once the required yield stress and time are reached the onset of crazing occurs, leading to dilatational elongation of the sample. The energy which is applied to the sample is absorbed by the formation of localized regions of high orientation and low density. Optical micrographs, taken between crossed polars,

of samples similar to those in *Figure 2* are shown in *Figure 3*. In this figure virgin PS can be compared with the HIPS sample. In virgin PS (*Figure 3a*) a sharp conchoidal fracture surface reflects brittle failure, and crazes are seen to diverge from the failed surface. The HIPS sample fails ductilely with a highly deformed failure surface. Crazes are so numerous in the HIPS sample that the micrograph produced between crossed polars is opaque (see *Figure 3f*). Crazes form at 90° to the stress direction which is indicated by the large arrow. It has been proposed that there is a minimum size beyond which a craze will degenerate into a crack. The effect of the added rubbery domains in HIPS is to increase the number of crazes, which decreases the average length, thereby delaying the onset of failure.

The stress/strain curve of *Figure 2d* shows subtle differences from that of HIPS. For example, the initial linear modulus is reduced from that of PS and HIPS, which indicates plasticization of the matrix phase. Furthermore, the material shows a gradual reduction in modulus before a broad yield point occurs. A yield point followed by a drop in stress is not expected for materials which exhibit shear banding in the absence of crazes¹. *Figure 3e* is of a recently failed sample with a stress/strain behaviour similar to that shown in *Figure 2d*. In addition to crazes, which occur at 90° to the stress direction (indicated by the horizontal arrow), shear bands appear at 45° to the stress direction, along the principle planes of stress. Under cross polars these highly oriented regions appear as bright lines. At many of the intersection points between crazes and shear bands crystalline

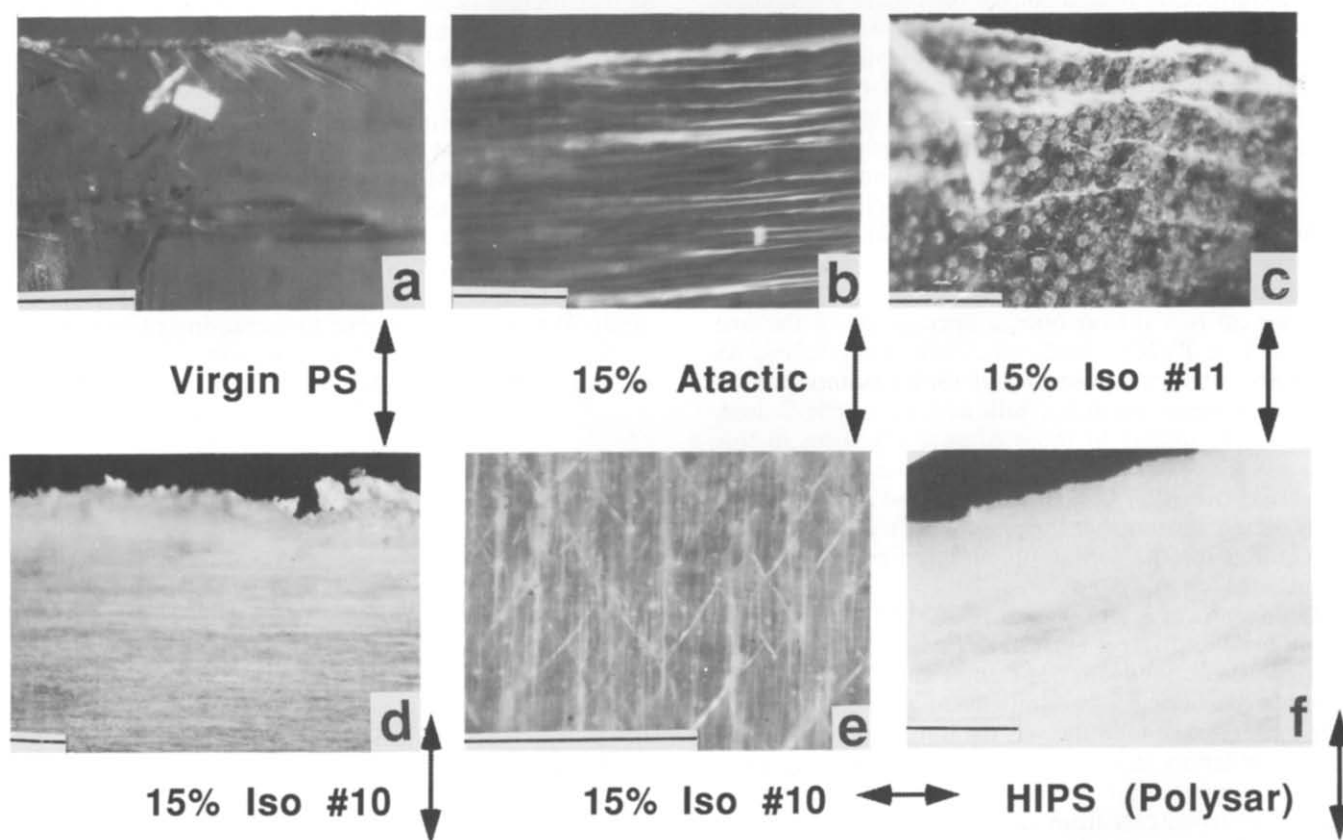


Figure 3 Optical micrographs of solution-cast samples taken under crossed polars where regions of high birefringence, such as those due to orientation or crystallinity, appear bright: (a) virgin PS; (b) 15 wt% atactic PVME/PS blend; (c) 15 wt% isotactic PVME/PS blend with large crystalline domains ($25 \mu\text{m}$); (d) 15 wt% isotactic PVME/PS blend with crystalline domains of $1\text{--}5 \mu\text{m}$, showing surface aged for 24 h after failure; (e) bulk sample of blend as in (d), taken immediately after failure and; (f) HIPS. Stress directions are indicated by arrows; scale bar = $200 \mu\text{m}$

domains of PVME show up as bright spheres. There is a dispersity in sphere size with spheres of approximately $5\ \mu\text{m}$ being most predominant at the intersection points. Returning again to *Figure 2d* it is possible that the initial lowering of the linear modulus before the broad yield point is due to the formation of shear bands, since both features are absent in the HIPS sample. As noted above, this shear banding may be enhanced by the thinness of the films, although shear banding is absent in the HIPS cast film and in the atactic blends.

Shear bands are known to exhibit relaxation¹. This behaviour is clearly observed in the shear banded blends that have been studied. *Figure 3d*, showing the failed surface, was taken a day after failure. *Figure 3e* was taken immediately after failure. In the aged sample the shear bands have relaxed. This effect was previously observed for shear bands and was used as evidence that molecular cohesion is retained in these bands. On the other hand, crazes are said to destroy molecular cohesion and therefore do not show this relaxation behaviour. The deformation behaviour shown in the shear banded PVME blend is reminiscent of the deformation behaviour displayed by SBR toughened PS, i.e. $\sim 50\%$ crazing and $\sim 50\%$ shear band deformation^{5,22-24}.

After drawing to large elongations, crazing occurs both in HIPS and in the material of *Figure 2d*. In both of these materials a large number of small crazes appear in the micrographs. It is believed that the yielding/drawing behaviour and the occurrence of crazes are related. The yield point in HIPS (see *Figure 2e*) and in the *i*PVME/PS blend of *Figure 2d* reflects the stress level necessary for the formation of crazes³⁷. For the material of *Figure 2d* the initial stress level for the formation of crazes is slightly lower, and occurs over a longer time-scale when compared with HIPS. The broadened yield region may be due to inhomogeneities in the modulus which are caused by shear banding of the partially yielded matrix phase. In *Figure 2d*, crazes are limited in size by termination or initiation at both rubber phases and at shear bands. The micrograph of the failed '15% Iso #10' surface (*Figure 3d*) shows that the material fails ductilely with a highly deformed failure surface. This should be compared with the less deformed surface of HIPS (*Figure 3f*) and the brittle surface of virgin PS (*Figure 3a*).

Figure 3b is a similar optical micrograph of the one phase atactic PVME blend, which is non-crystalline. As noted above with respect to *Figure 2b* this material shows a reduced linear modulus, followed by brittle failure. Crazes, very similar to those of pure PS, form in this material. However, no evidence for shear banding is observed. A brittle, failed surface is also shown. From these data it appears that the presence of a disperse phase is required for the formation of shear bands in these blends.

Figure 3c is of a higher tacticity PVME (#11) blend, which produced larger crystalline phases of $\sim 25\ \mu\text{m}$. In this case shear bands do not form. Failure occurs at the interface between phases, thus leading to large cracks. The initial tensile modulus, i.e. the initial slope in *Figure 2c*, is similar to that of pure PS, indicating a greater degree of immiscibility which is due to crystallization in this blend when cast from solution. Owing to differing initial solvent evaporation rates and other factors not completely under experimental control a comprehensive study of the relationship between phase size and mechanical properties could not be performed. With the

synthesis of larger quantities of isotactic PVME attention was shifted to melt blended samples.

Melt blended samples

Isotactic PVME is melt blended with Polysar[®] polystyrene with a molecular weight, $M_w = 395\ \text{kg mol}^{-1}$ ($M_w/M_n \sim 2$). The blends are produced by melt blending in the miscible region ($\sim 120^\circ\text{C}$), followed by pressing above the cloud point temperature ($\sim 156^\circ\text{C}$). None of these melt blends show the drastic improvement in mechanical properties observed for some of the solution-cast samples. Shear bands are not observed in the failed samples, although it is difficult to examine these thick samples using optical microscopy. Thin samples obtained from the mould flashing also fail to show shear banding after deformation. Isotactic PVME domains in the phase separated blends do not show strong birefringence, indicating that the domains are not significantly crystalline. Similarly, differential scanning calorimetry and X-ray diffraction data do not display PVME crystallinity. Failure, in all of the melt blended samples, occurs by fairly localized crazing. In all of the samples, brittle failure occurs with a conchoidal failure surface.

Since yielding/drawing is the predominant energy absorption characteristic in the best solvent-cast samples, strain at failure is a good indication of the improvement in mechanical properties. *Figure 4* is a plot of strain at failure versus percentage PVME for melt blended, phase separated blends of atactic and isotactic PVME with PS. A slight improvement over the atactic blends is observed for the isotactic blends, but when compared to similarly prepared samples with HIPS the improvement is insignificant (see *Figure 5*). It is interesting to note that the addition of isotactic PVME to HIPS appears to improve the strain at failure. This is probably due to plasticization of the PS matrix by PVME, indicating miscibility for the PVME in this complex system. A maximum in the strain at failure occurs at about 15 wt% PVME for both the atactic and isotactic PVME/PS blends. X-ray diffraction (XRD) from the melt blended samples fails to show any traces of crystallinity in the PVME phase. Since blends with lower concentrations of PVME are more miscible at a fixed temperature (see later), the initial increase in strain at failure may be due to increasing plasticization of the matrix phase, i.e. at low percentages of PVME a substantial amount of the PVME goes into the matrix

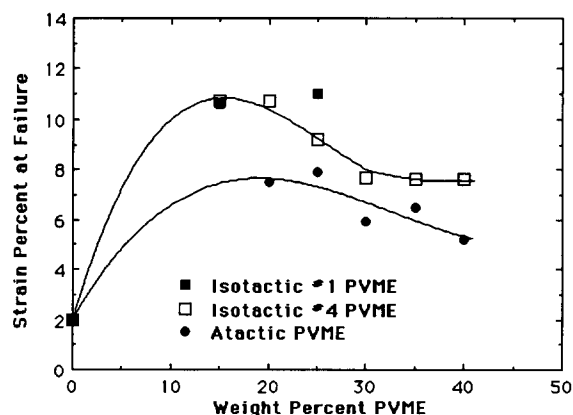


Figure 4 Plots of strain at failure versus weight percentage of PVME for phase separated blends of atactic (●) and isotactic (□, ■) PVME with PS

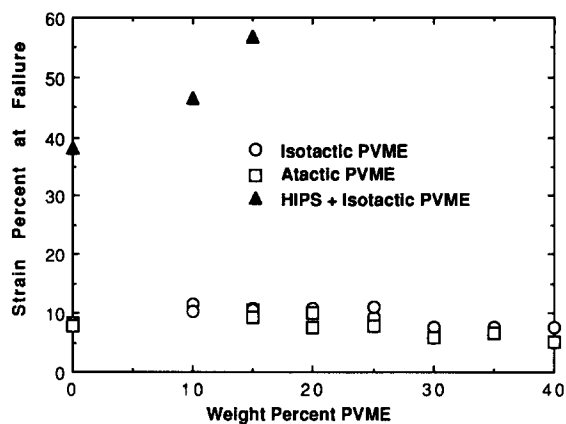


Figure 5 Strain at failure versus weight percentage of PVME in phase separated blends: (□) atactic PVME/PS, as in Figure 4; (○) isotactic PVME/PS, as in Figure 4 and; (▲) isotactic PVME/HIPS

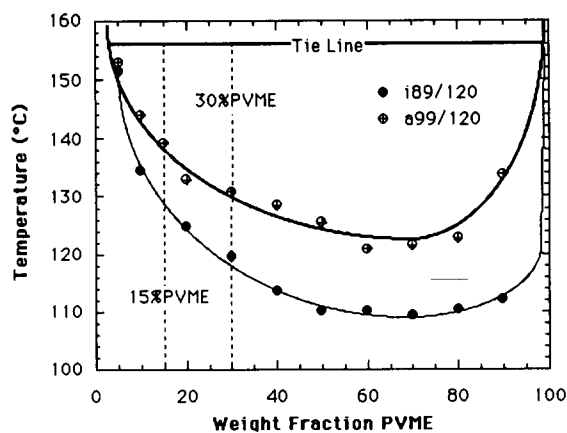


Figure 7 Phase diagram for isotactic and atactic PVME/PS blends. Lines are for clarity and do not reflect a fit

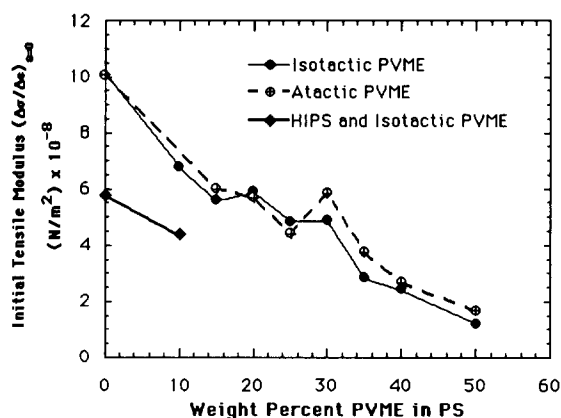


Figure 6 Initial modulus of the blends versus weight percentage of PVME: (●) isotactic PVME/PS; (⊕) atactic PVME/PS and; (◆) isotactic PVME/HIPS. Lines connect the data points for clarity only

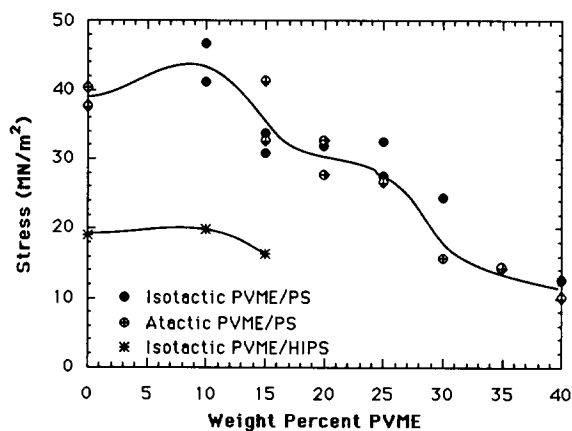


Figure 8 Plots of stress at failure versus weight percentage of PVME in various PVME/PS blends: (⊕) atactic PVME/PS; (●) isotactic PVME/PS and; (*) isotactic PVME/HIPS

phase. At PVME concentrations above 15 wt% this plasticization does not increase since the phase diagram levels off.

The initial modulus is a measure of the matrix phase modulus, as modified by plasticization, shear banding and to some extent, the structure of the two-phase material. Data on the initial modulus of the blends (Figure 6), shows a linear decrease in the initial tensile modulus with increased weight fraction of PVME of ~15 wt% PVME, followed by a trend towards levelling off between 15–30 wt% PVME. After the tendency towards a plateau in the 15–30 wt% PVME range, the modulus drops above 30 wt% PVME. The behaviour is consistent with the phase diagram (Figure 7), which drops rapidly in the low-concentration PVME region, i.e. below 15 wt% PVME. In the mid-composition range, i.e. 15–75 wt% PVME, the phase diagram is rather flat. Therefore, the low-concentration fall of the modulus is in a high miscibility region where a substantial amount of the added PVME plasticizes the matrix, leading to linear behaviour. At a level of ~15 wt% the majority of the additional PVME goes into the formation of phase separated domains, and the matrix composition remains fairly constant. Finally, at higher compositions of PVME, the PVME phases may begin to show continuity as the

PS-modified PVME becomes the majority phase. This should occur at about 52 wt% PVME, following the tie line shown in Figure 7, which is drawn at the temperature of melt blending.

The large scatter in the mechanical data make generalizations difficult. Figures 4–6 are compilations of a number of different blends made under various annealing conditions and with additives, such as 1 wt% of the heat stabilizer, Santonox White Crystals®, and 1 wt% crystallizing agents, such as silica or sodium benzoate, either present or absent. Small amounts of these additives have no effect on the mechanical tests. Annealing of the phase separated blends have slight effects, as discussed below.

Stress-at-failure data are presented in Figure 8. The PVME blends showed a failure stress comparable with pure polystyrene, which is shown at the (wt% PVME = 0) intercept in this figure. Data for HIPS blends with isotactic PVME (including pure HIPS) are shown for comparison. There is essentially no difference in the stress at failure for the isotactic and atactic melt blends. The stress at failure for the PVME blends shows a rise until ~10 wt% PVME. This demonstrates the effect of added non-crystalline domains and the plasticization effect at moderate percentages of PVME. Shear banding may be

a factor in this rise at low concentrations of PVME, although this cannot be demonstrated in the optical micrographs. The drop in stress at failure and the plateau in the 10–30 wt% range is reminiscent of the behaviour of the initial modulus. The behaviour of the stress at failure might be expected to follow the modulus in this way and similar reasoning could be applied to explain the behaviour. The HIPS blends show a less pronounced increase in the stress at failure at low concentrations of PVME, indicating the possibility of plastication-induced shear banding, although these cannot be observed in the blends, as a result of turbidity. At 25–30 wt% PVME a sharp drop in the stress at failure is observed, followed by a monotonic decrease above 35 wt%, although the data are less than conclusive. Such a drop in stress at failure might be related to changes in the stress field with differing blend structure, i.e. corresponding to the PVME phase becoming continuous.

The energy absorbed in the tensile tests is calculated from the areas under the stress–strain curves. Figure 9 shows that none of the PVME melt blends show an energy absorption which is comparable with HIPS. The absorbed energy behaves in a manner very similar to that of both the strain and stress. The initial increase in absorbed energy is probably due to plasticization. The plateau in the absorbed energy mimics the plateau region

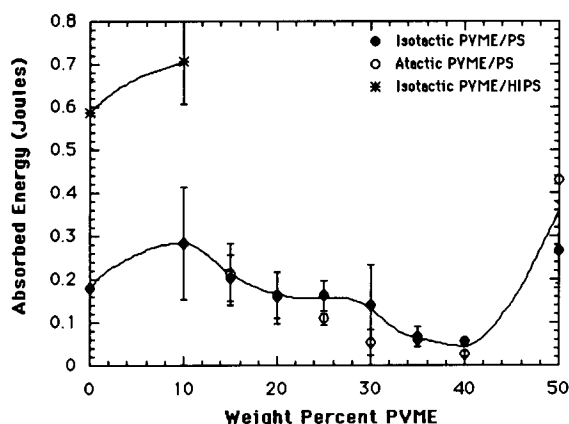


Figure 9 Absorbed energy versus weight percentage of PVME in various PVME/PS blends: (○) atactic PVME/PS; (●) isotactic PVME/PS and; (*) isotactic PVME/HIPS. Lines connect the data points for clarity only and do not reflect a fit

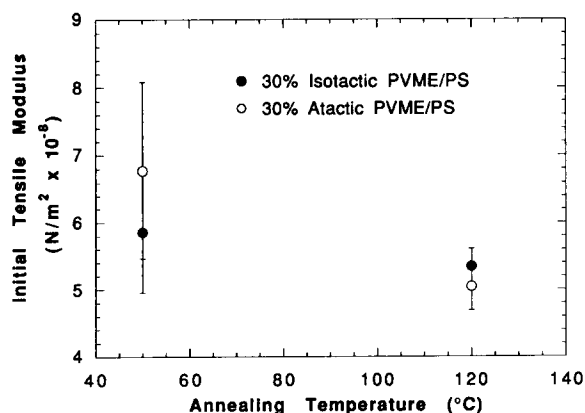


Figure 10 Initial modulus versus annealing temperature for 30 wt% PVME/PS blends: (○) atactic PVME and; (●) isotactic PVME

of the phase diagram (see Figure 7). The behaviour above 30 wt% PVME is believed to be due to various stages of PVME phase continuity. The 50 wt% PVME blend shows an anomalous increase in energy absorption, due to a large extension in the low-modulus material (see Figures 4 and 6). This increase in the absorbed energy and decrease in the modulus may be related to the PVME phase reaching continuity. Due to the thickness of the samples these postulates could not be proven by optical microscopy or light scattering measurements.

Annealing of the blends

In practice, it is impossible to drastically alter the final phase sizes or mechanical properties in the phase separated blends by either annealing or by pressing tensile bars at different temperatures. Generally, homogeneous phases, ~10 μm in size, with no detectable crystallinity, are produced, as estimated from crude optical microscopy of the mould flashing (which is fairly thin) and from XRD studies. This behaviour is probably due to the limitations of kinetic phenomena in the phase separation process.

Annealing is used first in an attempt to increase the crystallinity in the PVME phase with an annealing temperature of 50°C. The melting point for isotactic PVME occurs over a range of temperatures, depending on the annealing temperature, but is always observed between 40 and 70°C. The 50°C anneal (see Figure 10) is believed to be close to 20°C below the ideal melting point.

An attempt is next made to reduce the PVME phase size by annealing the blends below the phase separation temperature, by using an annealing temperature of 120°C. The initial modulus is a measure of the amount of PVME in the matrix phase. Figure 10 is an example of such attempts for the 30 wt% PVME blends. The glass transition temperature for the matrix phase in these blends is ~55°C. The large scatter in the data and lack of drastic effects are characteristic of the results. The tensile bars are annealed at 50°C for 8 days and at 120°C for 5 days. Generally, the isotactic blends showed higher absorbed energies, although these differences are within the scatter of the data. Annealing above the glass transition temperature of the blend yields a slightly lower modulus and a higher energy absorption, but the small differences may be due to relaxation of internal stresses that are present in the melt pressed blends. Annealing below 50°C, not shown in the figure, also fails to produce improved mechanical results. Annealing for longer periods is limited by the thermal stability of the PVME, even in the presence of antioxidants. It was found that blends annealed at 120°C for more than a week became brown.

Crystallization of *i*PVME

It is believed that the absence of crystallinity in the melt blended isotactic samples prevents the formation of a resilient rubbery phase, which appears to be necessary for improved toughness. The introduction of crystallizing agents, specifically sodium benzoate and silica, could improve the crystallinity of the rubbery phase. If the crystallization is limited by kinetics, rather than nucleation, these additives are expected to have little effect. This would be the case if high-molecular-weight PVME selectively fractionated to the PVME-rich phase. XRD is the most sensitive of the standard techniques that are available to observe small amounts of crystallinity. Various amounts of crystallizing agents were added to pure PVME in order to increase the rate of nucleation.

The addition of crystallizing agents had no effect on the rate, or on the final degree of crystallinity. Generally, traces of crystallinity appear after about one day, and full crystallinity occurs after about two weeks at room temperature. This corresponds well with the development of mechanical resiliency in iPVME.

The annealing of iPVME at temperatures both above and below room temperature serves only to reduce the rate and amount of crystallinity. Melt blends which contain small amounts of crystallizing agents fail to show any differences in mechanical properties.

Further fractionation of the PVME is a route to increased isotacticity. PVME displays a *LCST* in water which can be used to reduce the polydispersity and increase the isotacticity. Isotactic PVME is much less miscible in water than atactic PVME. Repeated fractionation by heating an aqueous solution of the PVME, leading to solvent/polymer phase separation, followed by a solvent/non-solvent fractionation, using benzene as the solvent and heptane as the non-solvent, yielded PVME with a higher degree of isotacticity and a lower polydispersity. This material showed a slightly faster rate of crystallization. Melt blends of this isotactic PVME failed to show improved mechanical properties or crystallinity in the iPVME phase. The multiply fractionated PVME had a slightly higher molecular weight than the original material.

Effect of added solvent

Small amounts of toluene were added to the melt blended samples during mixing in an attempt to aid the crystallization of the isotactic PVME. These blends failed to show improved mechanical behaviour. In no case are shear bands observed for these melt/solvent blended samples.

CONCLUSIONS

Isotactic PVME/PS blends, produced by the solution-casting of relatively thin films, show in some cases the presence of shear bands and extensive crazing. In these materials dramatic increases in the tensile stress, the strain at failure and the energy absorption are found to occur. A combination of plasticization of the matrix phase by the miscible PVME, and the presence of resilient crystalline PVME domains of $\sim 5 \mu\text{m}$ in size, appear to be necessary conditions for this toughening mechanism. Phase separation for the solution-cast samples is driven by crystallization of the isotactic PVME during evaporation of the solvent. The solution crystallized blends have a final morphology which mimics the morphology discussed with reference to *Figure 1*.

Attempts were made to produce similar materials following the scheme outlined in *Figure 1*, i.e. by melt blending in the miscible region and by pressing ASTM tensile bars above the phase separation temperature, followed by quenching. However, mechanical properties similar to those obtained by solution crystallization were not obtained. Isotactic PVME domains from the phase separated material in this case did not show crystallinity, either by differential scanning calorimetry, observation of birefringence under crossed polars, or by X-ray diffraction studies. Some degree of control over the mechanical properties was obtained by extensive annealing of the phase separated blends above their glass transition temperature and below their phase separation

temperature. Although this was successful in modifying the phase size, crystallinity was not produced in the isotactic PVME domains obtained from melt blended samples.

A study of the thermodynamics of phase separation in tactic PVME/PS blends using the Flory-Huggins-Staverman theory^{28,38-44} indicated that molecular-weight fractionation occurs in thermally induced phase separation from polydisperse polymer blends. This analysis predicted that only the highest-molecular-weight PVME goes to the PVME-rich domains. Such fractionation is believed to hinder crystallization in the melt blends that are discussed here. The presence of PS in the PVME-rich phase also served to inhibit iPVME crystallization. In contrast, crystallization-driven phase separation tended to select lower-molecular-weight polymer with a higher degree of isotacticity. Only limited amounts of the PS were incorporated into the iPVME crystalline domains. This explains the failure of the melt blended samples to produce crystalline PVME domains and mechanical properties that are similar to the solution-cast samples.

From the analysis given above we believe that polymer blends with improved mechanical properties can be produced in this system from melt blends if a low-dispersity, high-tacticity PVME of lower molecular weight is used.

The approach used in this paper assumes that physical crosslinking of the rubbery phase is a prerequisite for toughening in glassy polymers. This point is difficult to prove with the information available here. We can say that crystallinity is absent from the melt blends which do not show a toughening effect and is present in the blends which show this effect. However, other factors, such as the dilution of the PVME phase in the melt blended samples by PS, may account for the failure to produce significant toughening.

REFERENCES

- 1 Bucknall, C. B. 'Toughened Plastics', Applied Science, London, 1977, Ch. 1
- 2 Bucknall, C. B. 'Toughened Plastics', Applied Science, London, 1977, p. 100
- 3 Bucknall, C. B. *Makromol. Chem. Macromol. Symp.* 1990, **38**, 1
- 4 Keskkula, H. *Adv. Chem. Ser.* 1989, **222**, 289
- 5 Ku, P. L. *Adv. Polym. Technol.* 1988, **8**, 201
- 6 Rudolph, H. *Makromol. Chem. Macromol. Symp.* 1988, **16**, 57
- 7 Seymour, R. B. *Popular Plast.* 1988, **32**, 32
- 8 Echte, A. *Polym. Mater. Sci. Eng.* 1987, **57**, 542
- 9 Bucknall, C. B. in 'Polymer Blends and Mixtures' (Eds D. J. Walsh and J. S. Higgins), NATO ASI Series E No. 89, Martinus Nijhoff, Dordrecht, 1985, p. 363
- 10 Platzer, N. *Chemtech* 1977, **7**, 634
- 11 Amos, J. L. *Polym. Eng. Sci.* 1974, **14**, 1
- 12 Bowden, M. J. *Proc. Aust. Chem. Inst.* 1971, **38**, 190
- 13 Stone, R. W. *Br. Plast. (Special Suppl.)* 1971, **60-63**, 65
- 14 Braun, D. B. *Makromol. Chem. Macromol. Symp.* 1989, **29**, 73
- 15 Rudolph, H. *Makromol. Chem. Macromol. Symp.* 1988, **16**, 57
- 16 McMurrer, M. C. *Plast. Compounds* 1983, **6**, 77, 80, 84, 86
- 17 Naitove, M. H. *Plast. Technol.* 1975, **21**, 48
- 18 Peacock III, L. W. and Lutz Jr, J. T. *Plast. Eng.* 1977, **33**, 36
- 19 Sahajpal, V. in 'Developments in PVC Technology' (Eds J. H. L. Henson and A. Whelan), Wiley, New York, 1973, p. 62
- 20 McCarthy, J. P. in 'Compalloy '90', Proceedings of 2nd International Congress on Compatibility of Reactive Polymers and Alloying (Ed. J. A. Mason), Schotland Business Research, Princeton, NJ, 1990, p. 461
- 21 Liegeois, J. M., Hoff, J. P. and Kaesmacher, B. *Polym. Mater. Sci. Eng.* 1990, **63**, 215
- 22 Argon, A. S. and Cohen, R. E. *Adv. Polym. Sci.* 1990, **91/92**, 301

Study of iPVE/PS blends: G. Beaucage and R. S. Stein

- 23 Heggs, T. G. in 'Block Copolymers' (Ed. D. C. Allport), Wiley, New York, 1973, p. 493
- 24 Durst, R. R., Griffith, R. M., Urbanic, A. J. and van Essen, W. J. *Am. Chem. Soc. Div. Org. Coatings Plast. Prepr.* 1974, **34**, 320
- 25 Beaucage, G. and Stein, R. S. *U.S. Patent 07/895,413*
- 26 Beaucage, G. *PhD Dissertation* University of Massachusetts, Amherst, 1991
- 27 Beaucage, G., Stein, R. S., Hashimoto, T. and Hasegawa, H. *Macromolecules* 1991, **24**, 3443
- 28 Beaucage, G., Koningsveld, R. and Stein, R. S. *Macromolecules* 1993, **26**, 1603
- 29 Beaucage, G. and Stein, R. S. *Macromolecules* 1993, **26**, 1609
- 30 Beaucage, G. and Stein, R. S. *Macromolecules* 1993, **26**, 1617
- 31 Beaucage, G., Stein, R. S., Composto, R., Satkowski, M. S., Smith, S., Hamilton, W. and Smith, G. *Langmuir* submitted
- 32 Bank, R., Leffingwell, J. and Thies, C. *Am. Chem. Soc. Div. Polym. Chem. Polym. Prepr.* 1969, **10**, 622
- 33 Yang, S. *PhD Dissertation* University of Massachusetts, Amherst, 1981
- 34 Hashimoto, T., Kumaki, J. and Kawai, H. *Macromolecules* 1983, **16**, 641
- 35 Shibayama, M., Yang, H., Stein, R. S. and Han, C. C. *Macromolecules* 1985, **18**, 2179
- 36 This is true for all monosubstituted vinyl polymers, see Karasz, F. E. and MacKnight, W. J. *Macromolecules* 1968, **1**, 537
- 37 Bucknall, C. B. 'Toughened Plastics', Applied Science, London, 1977, p. 172
- 38 Staverman, A. J. *Rev. Trav. Chim. Pays-Bas* 1937, **56**, 885
- 39 Bondi, A. *J. Phys. Chem.* 1964, **68**, 441
- 40 Beckman, E. J., Porter, R. S. and Koningsveld, R. *J. Phys. Chem.* 1987, **91**, 6429
- 41 Koningsveld, R. and Staverman, A. J. *J. Polym. Sci. (Part A-2)* 1968, **6**, 305, 325, 349
- 42 Koningsveld, R. and Staverman, A. J. *Kolloid Z. Polym.* 1968, **218**, 114
- 43 Koningsveld, R. *Adv. Colloid Interface Sci.* 1968, **2**, 151
- 44 Koningsveld, R. *Discuss. Faraday Soc.* 1970, **49**, 144